

Superconductivity suppression of $\text{Ba}_{0.5}\text{K}_{0.5}\text{Fe}_{2-2x}\text{M}_{2x}\text{As}_2$ single crystals by substitution of transition metal ($M = \text{Mn, Ru, Co, Ni, Cu, and Zn}$)

J. Li,^{1,2,*} Y. F. Guo,^{1,3} S. B. Zhang,^{1,3} J. Yuan,¹ Y. Tsujimoto,³ X. Wang,^{1,2} C. I. Sathish,^{1,2} Y. Sun,³ S. Yu,¹ W. Yi,³ K. Yamaura,^{1,2,4} E. Takayama-Muromachiu,^{2,3,4} Y. Shirako,⁵ M. Akaogi,⁵ and H. Kontani⁶

¹*Superconducting Properties Unit, National Institute for Materials Science, 1-1 Namiki, Tsukuba, Ibaraki 305-0044, Japan*

²*Department of Chemistry, Graduate School of Science, Hokkaido University, Sapporo, Hokkaido 060-0810, Japan*

³*International Center for Materials Nanoarchitectonics (MANA), National Institute for Materials Science, 1-1 Namiki, Tsukuba, Ibaraki 305-0044, Japan*

⁴*JST, Transformative Research-Project on Iron Pnictides (TRIP), 1-1 Namiki, Tsukuba, Ibaraki 305-0044, Japan*

⁵*Department of Chemistry, Gakushuin University, 1-5-1 Mejiro, Toshima-ku, Tokyo 171-8588, Japan*

⁶*Department of Physics, Nagoya University, Furo-cho, Nagoya 464-8602, Japan*

(Received 8 February 2012; revised manuscript received 29 April 2012; published 11 June 2012)

We investigated the doping effects of magnetic and nonmagnetic impurities in single-crystalline p -type $\text{Ba}_{0.5}\text{K}_{0.5}\text{Fe}_{2-2x}\text{M}_{2x}\text{As}_2$ ($M = \text{Mn, Ru, Co, Ni, Cu, and Zn}$) superconductors. The superconductivity is maintained robustly with the impurity Ru, and weakly with the impurities Mn, Co, Ni, Cu, and Zn. However, the present T_c suppression rate of both magnetic and nonmagnetic impurities remains much lower than what was expected for the s_{\pm} -wave model. The temperature dependence of resistivity data shows an obvious low- T upturn for the crystals doped with high levels of impurity, which is due to the occurrence of localization. Thus, the relatively weak T_c suppression effect from Mn, Co, Ni, Cu, and Zn is considered to be a result of localization rather than the pair-breaking effect in the s_{\pm} -wave model.

DOI: [10.1103/PhysRevB.85.214509](https://doi.org/10.1103/PhysRevB.85.214509)

PACS number(s): 74.62.Bf, 74.25.Dw, 74.70.Dd

I. INTRODUCTION

The existence of the Fe-based superconductor family aroused unexpected rapid development,¹⁻³ not only because it is a second class of high- T_c superconductors after the cuprate superconductors, but also because it offers promise to understand the superconductivity (SC) mechanism of high- T_c superconductors by comparing the two families. Currently, it is probably the most crucial issue to confirm the pair-symmetry of the newly discovered superconductors, for which theoretical scientists proposed several possible models just after their discovery, among which the multigapped s -wave model is generally accepted, including the s_{\pm} ⁴⁻⁶ and s_{++} waves.⁷⁻⁹ Both states represent the same Fermi hole pockets, while they have opposite signs for the electron pockets; namely, the s_{\pm} wave is identified as a sign-reversal s -wave model, while there is a no sign reversal for the s_{++} state. Recently, results from various experiments failed to reach consensus for identifying which state represents the real nature of this superconductor.¹⁰⁻¹² Meanwhile, the d -wave model with opposite signs for the nearest-neighbor electron pockets still competes with other models, once there are nodes on the hole pockets or even on both the electron and hole pockets.^{6,13,14} More recent results suggested that different systems in the iron-pnictide family may represent different pair-symmetry types, even that the pair symmetry can be quite different from material to material.¹² The varieties of the possible scenarios have inspired further investigations, among which the use of impurity substitution is one of the most promising ways to address the issue and even to uncover competing orders, because the pair-breaking mechanism from both magnetic and nonmagnetic impurities should be different for these models.

The iron-pnictide superconductors commonly contain Fe_2X_2 ($X = \text{As, P, or Se}$) planes, which are well known as

the superconducting layers. The substitution of point defect impurities for Fe is introduced to understand the physical properties, similar to what was comprehensively studied in cuprates. According to Anderson's theorem, the nonmagnetic impurity (NMI) cannot break pairing in an isotropic SC gap, but can for an anisotropic gap,¹⁵ while the pair-breaking effect of the magnetic impurities is independent of gap type. Thus, the nonmagnetic point defects are of great importance. Zn^{2+} with a tightly closed d shell is preferred as an ideal NMI.¹⁶ Typically, Zn substitution for Cu was carried out over the last two decades on the cuprate superconductors such as $\text{YBa}_2\text{Cu}_3\text{O}_{7-\delta}$,¹⁶⁻¹⁸ $(\text{La,Sr})_2\text{CuO}_4$,^{16,19-21} and $\text{Bi}_2\text{Sr}_2\text{CaCu}_2\text{O}_8$.^{16,22-24} A few at.% of Zn acts as a strong scattering center and remarkably depresses SC due to the d -wave anisotropic gap for cuprates.¹⁶⁻²⁴ Since the doped Zn often plays a crucial role of pairing symmetry determination in previously known superconductors, we may expect that it works with the Fe-based superconductors as well.

Previous Zn studies for the Fe-based superconductors seem to be contradicted: Cheng *et al.* reported that the doped Zn hardly affects SC of the p -type $\text{Ba}_{0.5}\text{K}_{0.5}\text{Fe}_2\text{As}_2$,²⁵ as Li *et al.* did with $\text{LaFeAsO}_{0.85}\text{F}_{0.15}$.²⁶ However, we found that the SC was completely suppressed by at most 3 at.% of Zn for $\text{LaFeAsO}_{0.85}$ using a high-pressure method.²⁷ A comparable result was obtained in the $\text{K}_{0.8}\text{Fe}_{2-y-x}\text{Zn}_x\text{Se}_2$ superconductors.²⁸ Since the Zn substitution generally suffered from issues of low melting point and high volatility,^{23,24} it is uncertain whether Zn has been successfully substituted into the Fe site for polycrystals previously synthesized at ambient pressure. Our recent studies indeed showed that hardly more than 2 at.% of Zn was doped into the n -type $\text{Ba}(\text{Fe,Co})_2\text{As}_2$ superconductor at an ambient-pressure condition.²⁹ In contrast, linear T_c suppression was found for the high-pressure prepared $\text{BaFe}_{2-2x-2y}\text{Zn}_{2x}\text{Co}_{2y}\text{As}_2$ superconductors.³⁰ To avoid

overestimation of the net Zn, we proposed growing highly Zn-doped single crystals of the Fe-based superconductor by using a high-pressure technique.

In this study, we studied the impurity effect on the p -type (Ba,K)Fe₂As₂ superconductors using a high-pressure and high-temperature method, for which magnetic and nonmagnetic elements around Fe were selected as the dopant, including 3d metals Mn, Co, Ni, Cu, and Zn, and Ru from 4d. The specific heat, magnetic, and transport properties indicate that the SC is maintained robustly with the impurity Ru, and weakly with the impurities Mn, Co, Ni, Cu, and Zn.

II. EXPERIMENT

Single-crystalline samples of Ba_{0.5}K_{0.5}Fe₂As₂ (BK) and Ba_{0.5}K_{0.5}Fe_{2-2x}M_{2x}As₂ ($M = \text{Mn}, x = 0.02$ and 0.05 ; $M = \text{Ru}, \text{Co}, \text{Ni}, \text{Cu},$ and Zn , nominal $x = 0.05, 0.10,$ and 0.15) were prepared in a high-pressure apparatus as reported elsewhere.³⁰ Here the starting materials are BaAs (lab made), KAs (lab made), FeAs (lab made), Fe (3N), Mn (>99.9%), Ru (>99.9%), Co (>99.5%), Ni (>99.99%), Cu (>99.9%), and Zn (4N). Note that the pellets were self-separated into sizes of around $0.3 \times 0.2 \times 0.1 \text{ mm}^3$ or much smaller after being left in vacuum for 2–3 days. The selected single crystals were held on a MgO substrate with ab plane parallel to the substrate, and then cleaved into thin slices along the c axis as discussed in an earlier report.³⁰ To confirm the impurity substitution, the crystals were measured in an electron probe micro-analyzer (EPMA, JXA-8500F, JEOL) soon after being cleaved. Table I gives the real value of x for Ba_{0.5}K_{0.5}Fe_{2-2x}M_{2x}As₂ ($M = \text{Mn}, \text{Ru}, \text{Co}, \text{Ni}, \text{Cu},$ and Zn) with a starting value of $x = 0.05$. The result demonstrates little difference from the starting materials, although it shows a slightly lower concentration for Mn, Ru, Ni, and Zn. However, we will use the real concentration of x for the following analysis.

The cleaved single crystals were also studied by the x-ray diffraction (XRD) method in a Rigaku Ultima-IV diffractometer using Cu $K\alpha$ radiation. The single crystals were also ground and studied by a powder XRD method, and the results indicated that the tetragonal ThCr₂Si₂-type structure ($I4/mmm$) is formed over the compositions without a second phase.^{2,31}

In the dc magnetic susceptibility (χ) measurement, since the size of an individual crystal is too small to obtain accurate measurements, we loosely gathered small crystals (~ 30 mg in

total) into a sample holder, and measured them in a Magnetic Properties Measurement System by Quantum Design. The sample was cooled down to 2 K without applying a magnetic field (zero-field-cooling, ZFC), followed by warming to 45 K in a field of 10 Oe and then cooled down again to 2 K (field-cooling, FC).

The cleaved single crystals were used for the in-plane dc electrical resistivity (ρ_{ab}) measurement. To minimize the structure defects of the single crystals, we cleaved the crystals to $\sim 1\text{--}10 \mu\text{m}$ in thickness and cut them into quadrate shaped slices $\sim 100 \times 50 \mu\text{m}^2$. Then four terminals were created on the cleaved ab plane with platinum wires attached using silver paste. The ρ_{ab} was measured between 2 and 300 K in a Physical Properties Measurement System model 9 T (PPMS-9T) by Quantum Design. For such cleaved single crystals, the Hall coefficient (R_H) was also measured in the PPMS, where the electric current was along the ab plane and H was applied parallel to the c axis. For each sample of 12–14 mg of crystals, we measured the specific heat (C_p) in the PPMS-9T from 2 to 300 K by a heat-pulse relaxation method.

III. RESULTS AND DISCUSSION

A. X-ray diffraction

The XRD patterns for the cleavage plane of the separated crystals of Ba_{0.5}K_{0.5}Fe_{1.9}M_{0.1}As₂ ($M = \text{Fe}, \text{Mn}, \text{Ru}, \text{Co}, \text{Ni}, \text{Cu},$ and Zn , which are abbreviated as BK, BK-Mn, BK-Ru, BK-Co, BK-Ni, BK-Cu and BK-Zn, respectively) are shown in Fig. 1(a). The obvious orientation toward $[0\ 0\ 2n]$ (n is an integer) indicates that the cleavage plane is the ab plane of the ThCr₂Si₂-type structure. Note that the main peak (0 0 8) for every impurity-doped crystal indicates an obvious shift in 2θ as shown in Fig. 1(b), suggesting that the impurities were indeed doped into the crystal lattice. The lattice parameters obtained by assuming the same structure for the powder XRD data are summarized in Table I, where it can be seen that the impurity doping results in a change of both lattice parameters a and c . The unsystematic change in peak shift and lattice parameters seems unlikely to be due to the basic change in the size of doping ions. However, the difference between Fe-As and M-As bond size was considered a crucial factor, as discussed in Ref. 15. In addition, a magnetic effect is possibly included in the c -axis expansion,³² especially for the nonmagnetic Zn ions, which results in nearly isotropic expansion for both a

TABLE I. The columns give the parameters (from left to right) of Ba_{0.5}K_{0.5}Fe_{2-2x}M_{2x}As₂ ($M = \text{Fe}, \text{Mn}, \text{Ru}, \text{Co}, \text{Ni}, \text{Cu},$ and Zn , nominal $x = 0.05$): real atomic concentration $M(x)$ from the EPMA measurement, lattice parameters a and c from powder XRD, T_{cp} from resistivity data, and $\Delta C_p/T_{cp}$. The samples of Ba_{0.5}K_{0.5}Fe_{2-2x}M_{2x}As₂ ($M = \text{Fe}, \text{Mn}, \text{Ru}, \text{Co}, \text{Ni}, \text{Cu},$ and Zn) are abbreviated to BK, BK-Mn, BK-Ru, BK-Co, BK-Ni, BK-Cu, and BK-Zn, respectively.

Samples	$M(x)$	a (Å)	c (Å)	T_{cp} (K)	$\Delta C_p/T_{cp}$ (mJ mol ⁻¹ K ⁻²)
BK		4.014(2)	13.298(2)	37.78	44.50
BK-Mn	0.039(2)	3.984(1)	13.196(3)	9.53	
BK-Ru	0.032(6)	4.051(1)	13.419(4)	37.14	73.49
BK-Co	0.052(2)	4.038(1)	13.383(4)	30.31	39.26
BK-Ni	0.039(4)	3.990(1)	13.229(1)	26.75	
BK-Cu	0.044(1)	3.970(1)	13.050(5)	22.29	
BK-Zn	0.040(2)	4.102(2)	13.322(3)	30.15	21.66

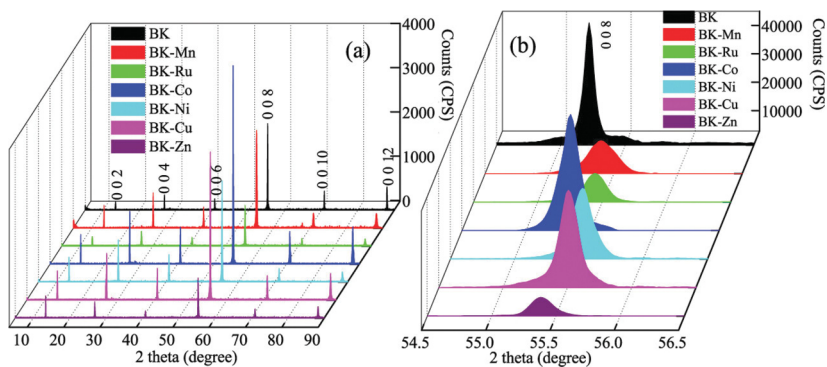


FIG. 1. (Color online) XRD pattern of single crystals of Ba_{0.5}K_{0.5}Fe_{2-2x}M_{2x}As₂ ($M = \text{Mn, Ru, Co, Ni, Cu, and Zn}$; real x values are shown in Table I).

and c . Comparably, Zn-doped BaFe_{1.91-x}Zn_xCo_{0.11}As₂³⁰ and YBa₂Cu_{3-3x}Zn_{3x}O_{7-δ}³³ also result in an isotropic expansion of the lattice.

B. Magnetic measurement

Figure 2 shows the T dependence of Ba_{0.5}K_{0.5}Fe₂As₂ and Ba_{0.5}K_{0.5}Fe_{2-2x}M_{2x}As₂ ($M = \text{Mn, Ru, Co, Ni, Cu, and Zn}$), where the impurity concentration of x is obtained from the EPMA measurements. The host crystal BK shows the maximum T_c of 38 K as reported elsewhere.² Obviously, the SC of Ba_{0.5}K_{0.5}Fe₂As₂ is maintained strongly with the Ru impurity, which is accordance with the previous studies of the Ru substitution effect in LaFeAsO_{1-x}F_x³⁴ and NdFeAsO_{0.89}F_{0.11} superconductors.³⁵ The magnetic impurity of Mn indicates the sharpest T_c suppression among all impurities. It is surprising that the T_c -reduction effects from the $3d$ transition metals

(Co, Ni, Cu, and Zn) are similar to each other, regardless of magnetic or nonmagnetic impurities.

C. Transport property

Transport properties provide direct information for the influence of impurities or defects on various SC properties, including the carrier properties, coupling between charges, spin degrees of freedom, and more importantly the pair-breaking symmetry.^{16,17} To obtain reliable transport data, high-quality single crystals are essential with substitution of impurities. Figure 3 shows the temperature dependence of ab -plane resistivity (ρ) for Ba_{0.5}K_{0.5}Fe_{2-2x}M_{2x}As₂ ($M = \text{Fe, Mn, Ru, Co, Ni, Cu, and Zn}$). The T_c was defined from the peak value for the plots of $d\rho/dT$ vs T . It is clearly observed that T_c goes down with substitution of Mn, Co, Ni, Cu, and Zn, while it is weakly suppressed by Ru, in good accordance with

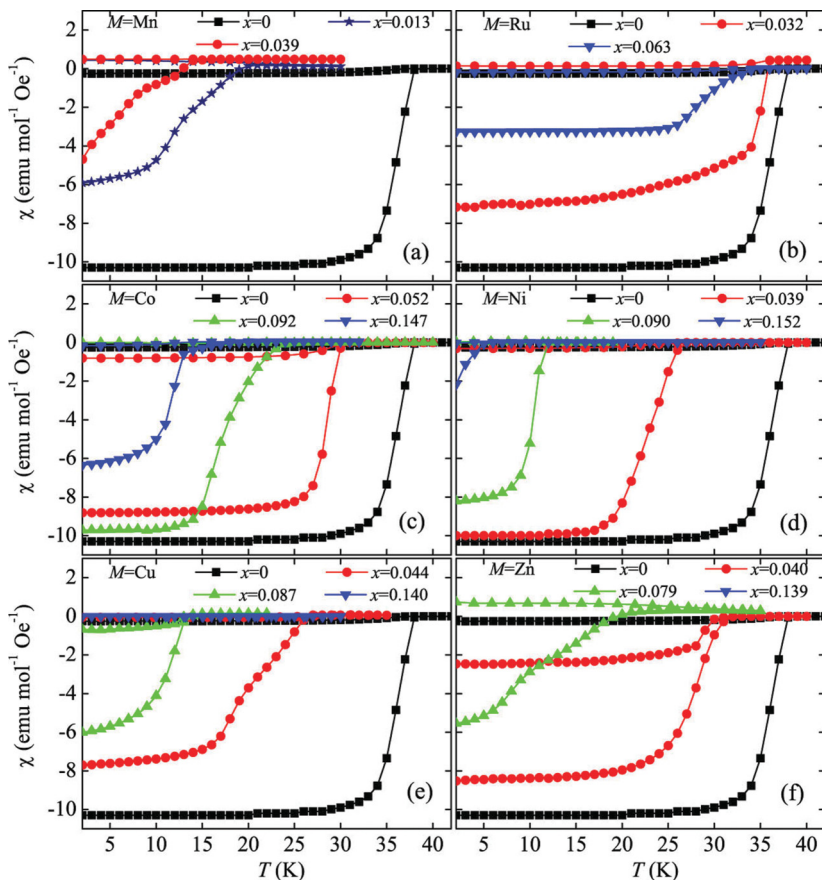


FIG. 2. (Color online) χ vs T for Ba_{0.5}K_{0.5}Fe_{2-2x}M_{2x}As₂ ($M = \text{Mn, Ru, Co, Ni, Cu, and Zn}$) at $H = 10$ Oe.

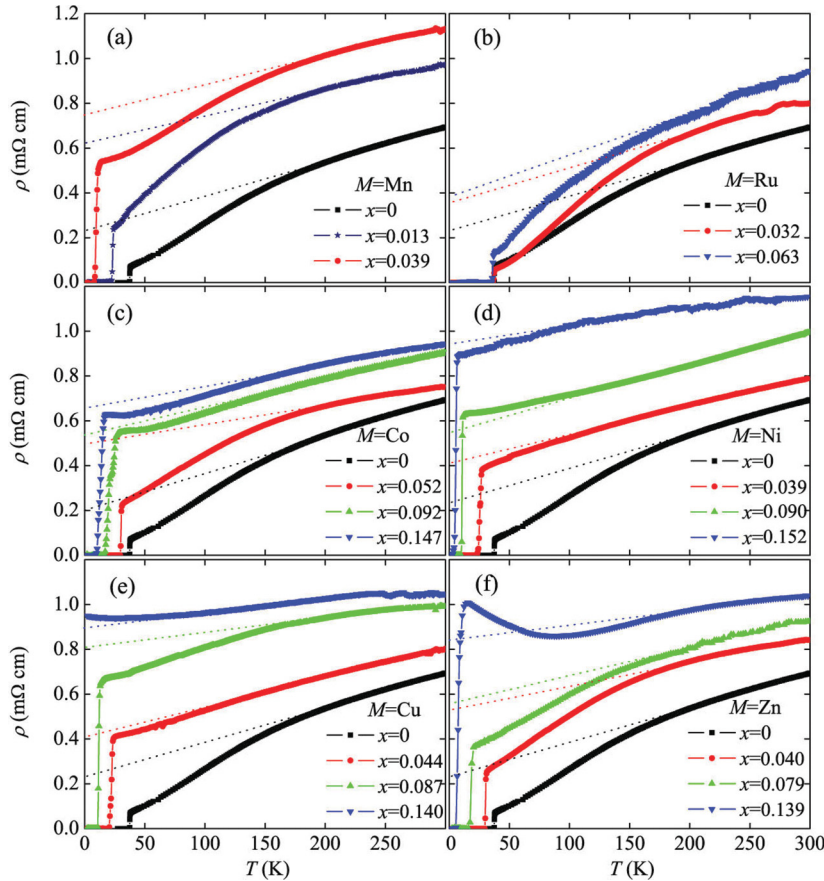


FIG. 3. (Color online) ρ vs T for $\text{Ba}_{0.5}\text{K}_{0.5}\text{Fe}_{2-2x}\text{M}_{2x}\text{As}_2$ ($M = \text{Mn, Ru, Co, Ni, Cu,}$ and Zn).

the magnetic results. Note that for $\text{Ba}_{0.5}\text{K}_{0.5}\text{Fe}_{2-2x}\text{Mn}_{2x}\text{As}_2$ ($x = 0, 0.013,$ and 0.039) the ρ - T curves are almost parallel to each other in the high- T region above T_c . Such behavior establishes that the hole content is modified by the defects rather than the electron irradiation. At low T on the other hand, an upturn in the ρ - T curve is observed with substitution of defect content ($x < 0.05$). This phenomenon has been often interpreted as the occurrence of localization. In case of Ru-doped crystals, the ρ - T curves show almost parallel upturn with substitution of Ru in both high- and low- T regions, suggesting the absence of localization. The ρ - T curves for the Co-, Ni-, Cu-, and Zn-doped crystals show no parallel shift from that of the impurity-free crystal. However, the low- T upturns of the resistivity appear for the impurity-doped crystals due to localization, regardless of magnetic or nonmagnetic impurities. Typically, the high-level Zn-doped crystals $\text{Ba}_{0.5}\text{K}_{0.5}\text{Fe}_{2-2x}\text{Zn}_{2x}\text{As}_2$ ($x = 0.139$) show a dramatic low- T upturn from localization. A similar phenomenon was observed in the Zn-substituted $\text{A}(\text{Fe,Zn,Co})_2\text{As}_2$ superconductors.^{30,36}

As the resistance of the superconductor shows a metal-like behavior, it decreases linearly with temperature in high-temperature regions. Therefore, we define the residual resistivity ρ_0 by the extrapolation of T vs linear resistivity to 0 K for the linear T dependence in the high- T region. The residual resistivity ρ_0 gradually increased with increasing doping level, except for Ru, and the rates of ρ_0 increase with x are $\sim 98.2, 22.3, 42.8, 46.2,$ and $35.1 \mu\Omega \text{ cm}/\%$ for Mn, Co, Ni, Cu, and Zn, respectively. The residual resistivity is due to defect scattering. Although it is not easy to obtain accurate

determinations of the scattering rate directly from resistivity data, an alternative approach is to seek information from the decrease of T_c induced by the scattering centers.¹⁶ Figure 4 shows the residual resistivity ρ_0 dependence of ΔT_c , where the T_c data are from resistivity measurements. The T_c is gradually suppressed with increasing ρ_0 for all impurities except Ru. The T_c is nearly independent of ρ_0 for the substitution of Ru, while it is suppressed by impurities Mn, Co, Ni, Cu, and Zn with suppression rates of 66.77, 76.78, 46.43, 51.67, and 59.45 K/ $\mu\Omega \text{ cm}$, respectively. Note that these impurities have similar suppression rates. However, the theoretical residual resistivity per 1% impurity with a delta-functional strong potential is just $\sim 20 \mu\Omega \text{ cm}$, and SC will also vanish with a

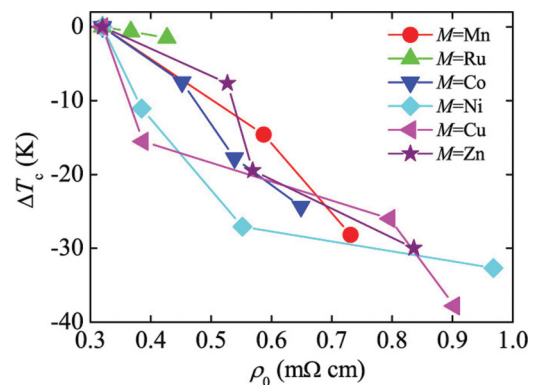


FIG. 4. (Color online) ΔT_c as a function of residual resistivity (ρ_0) for the superconductors $\text{Ba}_{0.5}\text{K}_{0.5}\text{Fe}_{2-2x}\text{M}_{2x}\text{As}_2$ ($M = \text{Mn, Ru, Co, Ni, Cu,}$ and Zn).

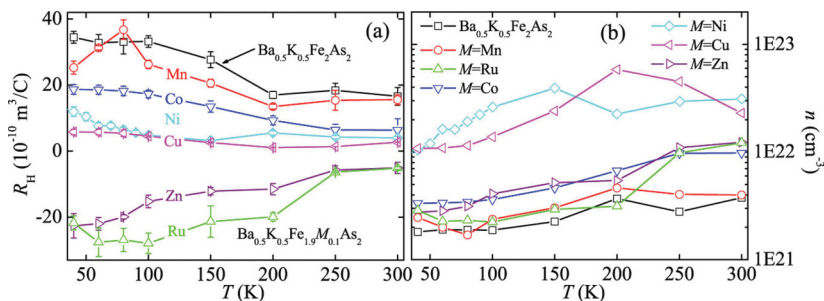


FIG. 5. (Color online) (a) Hall coefficient (R_H) vs T and (b) carrier density (n) vs T for single-crystalline $\text{Ba}_{0.5}\text{K}_{0.5}\text{Fe}_{2-2x}\text{M}_{2x}\text{As}_2$ ($M = \text{Fe, Mn, Ru, Co, Ni, Cu, and Zn}$; real x values are shown in Table I).

doping of 1% of either magnetic or nonmagnetic impurities for the s_{\pm} -wave model.⁷⁻⁹ Consequently, the suppression rate is around 1900 K/m Ω cm, indicating that the impurity scattering cross section is enlarged by the many-body effect, rather than the pair-breaking effect,^{37,38} which we will discuss in detail in Sec. IV.

Figure 5 shows the T dependence of the Hall coefficient (R_H) and carrier density (n) for the BK, BK-Mn, BK-Ru, BK-Co, BK-Ni, BK-Cu, and BK-Zn single crystals. The data for the impurity-free crystal are from Refs. 25 and 37. With substitution of 5 at.% of Mn, Co, Ni, or Cu, the BK crystal is observed to have slightly declining R_H , but increasing carrier density. Sato and co-workers^{10,34,35} proposed that the decrease in the absolute magnitude of R_H is due to the weakening of the magnetic fluctuations, as in the case of the thermoelectric power S . However, it is surprising that the impurities of Ru and Zn result in a negative R_H ; it seems likely that the introduction of Ru and Zn ions changes the charge carrier type from hole-doping to electron-doping. For the normal state, we found there is no significant change for various substitutions, indicating that the transition-metal substitution does not substantially alter the actual carrier density. This is

reasonable because the substitution is isovalent. Regarding the previous impurity effect on charge carriers of both Fe-based and Cu-based superconductors, fairly little change was observed in the R_H measurements as well.^{30,33} The actual carrier density change due to transition-metal impurities does not account for the systematic T_c decrease.⁵

D. Specific heat data

The temperature-dependent specific heats (C_p) in zero-field for BK, BK-Mn, BK-Ru, BK-Co, BK-Ni, BK-Cu, and BK-Zn are given in Fig. 6, where the inset of each figure demonstrates the derivation of C_p to T . An obvious heat capacity anomaly, indicated by arrows, is associated with the SC transition temperature for BK, BK-Ru, BK-Co, BK-Ni, and BK-Zn. However, there is almost no anomaly at T_c for BK-Mn and BK-Cu. It is possible that disorder regarding the impurity distribution causes inhomogeneous SC states, greatly broadening the expected peak, and the broad anomaly is masked by the lattice contributions.^{39,40} In addition, it was found that the character of the anomaly is strongly doping dependent.⁴¹ However, the reason for the absence of the

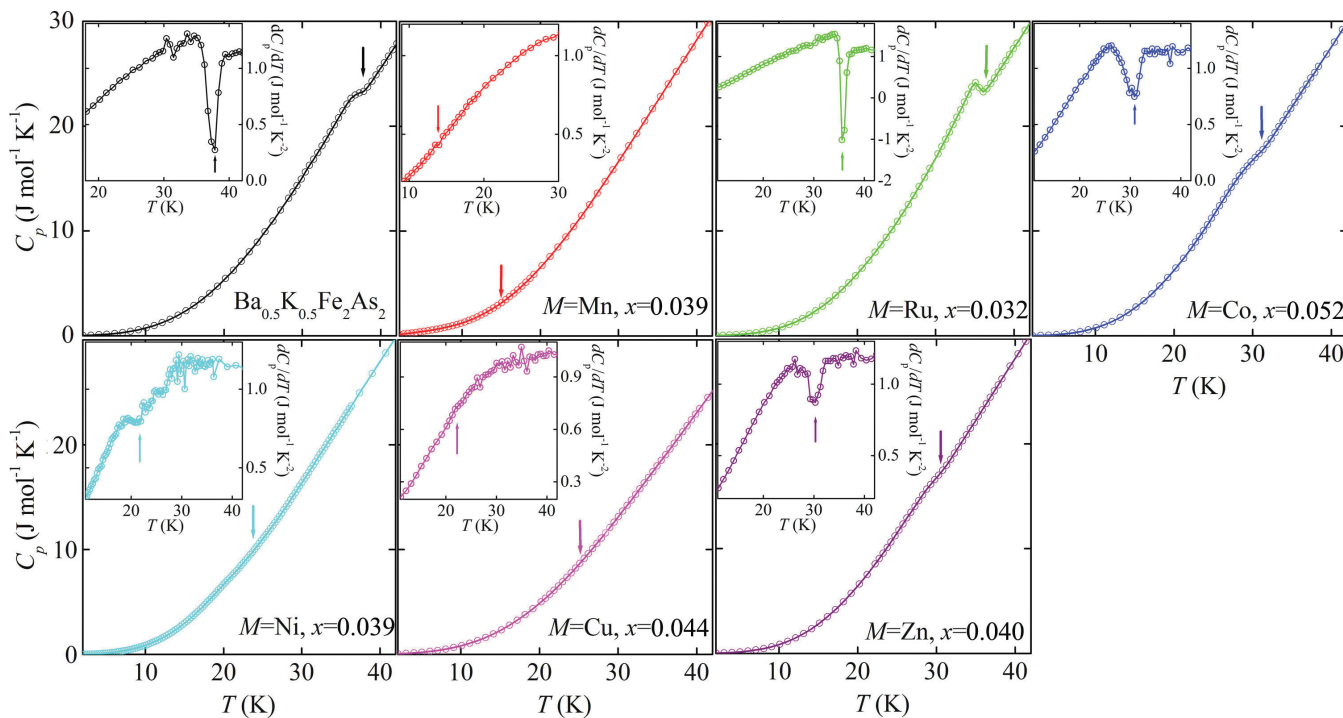


FIG. 6. (Color online) Specific heat dependence of the temperature for $\text{Ba}_{0.5}\text{K}_{0.5}\text{Fe}_{2-2x}\text{M}_{2x}\text{As}_2$ ($M = \text{Mn, Ru, Co, Ni, Cu, and Zn}$), where the inset of each figure demonstrates the derivation of C_p to T , and the arrows indicate the heat capacity anomaly.

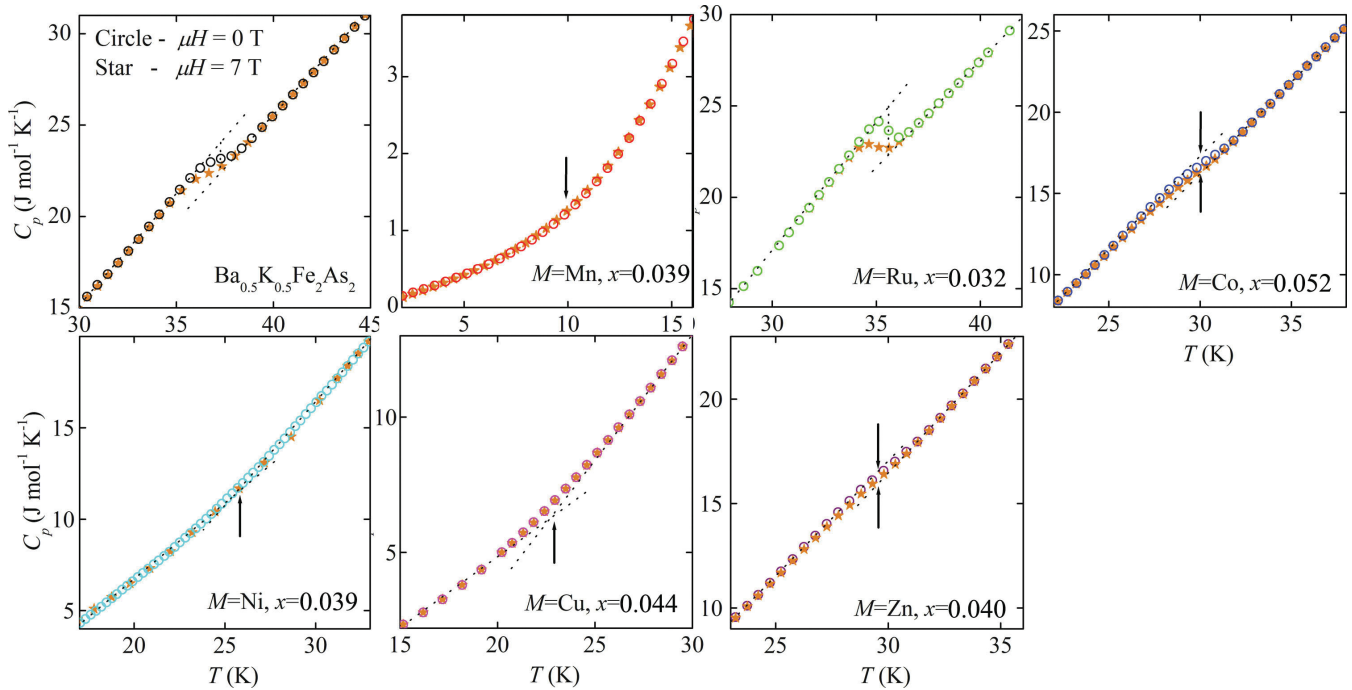


FIG. 7. (Color online) Specific heat dependence of the temperature for $\text{Ba}_{0.5}\text{K}_{0.5}\text{Fe}_{2-2x}\text{M}_{2x}\text{As}_2$ ($M = \text{Mn, Ru, Co, Ni, Cu, and Zn}$) with and without magnetic field of 7 T.

anomaly in Mn-, Ni-, and Cu-substituted samples needs further investigation. Figure 7 shows the C_p - T curves in fields of 0 and 7 T at around T_c , from which we estimate the specific heat jump ($\Delta C_p/T_{cp}$) for these transitions at zero-field, as shown in Table I, where T_{cp} is the T_c estimated from resistivity data. It is observed that the impurity substitutions yield a weak change in the superconducting phase as judged from the size of the specific heat jump, although the Co and Zn substitutions weakly reduced $\Delta C_p/T_{cp}$, and the Ru doping enhanced $\Delta C_p/T_{cp}$ (73.49 mJ mol⁻¹K⁻²) to about two times that of the impurity-free sample (44.50 mJ mol⁻¹K⁻²). On the other hand, the applied magnetic field of 7 T is not large enough to suppress the anomaly (see Fig. 7) due to the high upper critical fields (>55 T). Since both the superconducting temperature and the upper critical fields in these superconductors are relatively high, we can hardly make a reliable estimate of the normal-state electronic specific heat.

IV. DISCUSSION

We have described the influence of impurities on the magnetic, transport, and specific heat properties in the $\text{Ba}_{0.5}\text{K}_{0.5}\text{Fe}_2\text{As}_2$ superconductor. On basis of these results, we focus on the discussion of pair-breaking effects in terms of both s_{\pm} - and s_{++} -wave states.

Based on density functional calculations it was found that the impurity effects in iron-based superconductors can be classified into three groups according to the derived parameters: (i) Mn (0.3 eV), Co (-0.3 eV), and Ni (-0.8 eV); (ii) Ru (0.1 eV); and (iii) Zn (-8 eV).⁴² Among these impurities the nonmagnetic Zn works as a unitary scattering potential that is comparable to the bandwidth, with the result of a quite strong potential. Consequently, it is expected to have a strictly

pair-breaking effect on the anisotropic SC gaps. According to Ref. 7 the reduction in T_c due to a strong impurity potential in the s_{\pm} -wave state is $\sim 50z$ K/%, where z is the renormalization factor ($=m/m^*$; m and m^* are the band mass and the effective mass, respectively). The effective mass was estimated as $2m_e$ from ARPES in 122 superconductors;^{43,44} thus we obtain the suppression rate of 25 K/% for $z = 0.5$. In contrast, the T_c would be weakly suppressed by impurities in the s_{++} -wave state, due to the following reasons: (i) suppression of the orbital fluctuations, which is a possible origin of the s_{++} -wave state, because of the violation of the orbital degeneracy near the impurities, and (ii) the strong localization effect in which the mean free path is comparable to the lattice spacing.⁷ These may account for the observed T_c decrease. In our present results, the decrease of the χ and ρ -defined T_c ($T_{c\chi}$ and $T_{c\rho}$) with doping level x for the superconductors $\text{Ba}_{0.5}\text{K}_{0.5}\text{Fe}_{2-2x}\text{M}_{2x}\text{As}_2$ ($M = \text{Mn, Ru, Co, Ni, Cu, and Zn}$) is given in Fig. 8. We estimated

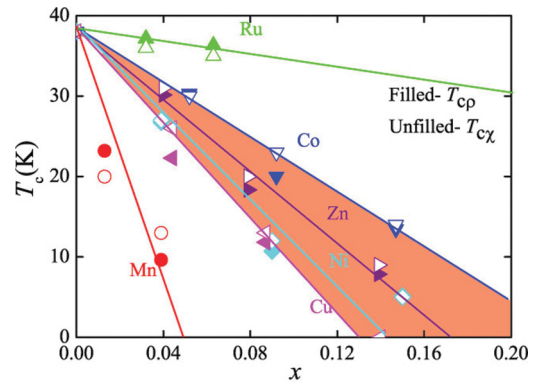


FIG. 8. (Color online) T_c vs x for the superconductors $\text{Ba}_{0.5}\text{K}_{0.5}\text{Fe}_{2-2x}\text{M}_{2x}\text{As}_2$ ($M = \text{Mn, Ru, Co, Ni, Cu, and Zn}$).

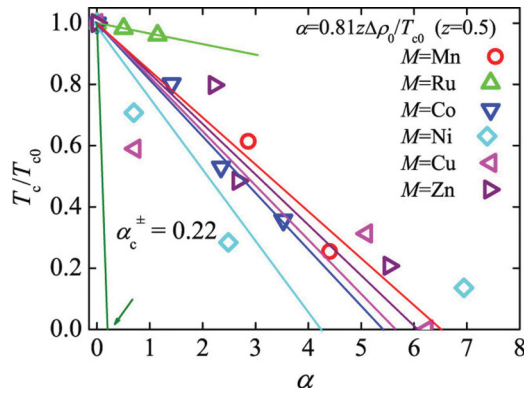


FIG. 9. (Color online) T_c/T_{c0} vs α with various calculations for Ba_{0.5}K_{0.5}Fe_{2-2x}M_{2x}As₂ ($M = \text{Mn, Co, Ni, Cu, and Zn}$). The T_c of each impurity-doped sample is normalized with T_{c0} of the impurity-free compound. The pair-breaking rate α is estimated as $\alpha = 0.88z\Delta\rho_0/T_{c0}$, where $\Delta\rho_0$ is the difference of the residual resistivity from that of impurity-free crystals, and z is the renormalization factor, for which we use $z = 0.5$ from the ARPES result for 122 superconductors.^{43,44}

the suppression rate of Zn as 2.22 K/% by applying a linear function to T_{cp} vs x , which is in good accordance with the BaFe_{1.89-2x}Zn_{2x}Co_{0.11}As₂ superconductors.³⁰ The observed robustness of SC seems likely to contradict the nonmagnetic impurity quantitatively in the s_{\pm} -wave model. Applying a linear function to T_{cp} vs x , the suppression rates for Mn, Ru, Co, Ni, and Cu are 6.98, 0.27, 1.73, 2.21, and 2.68 K/%, respectively. Among these impurities Mn is observed as having the strongest suppression effects, even though such as influence is much weaker than what was expected from the s_{\pm} -wave model. The negligible suppression effect from Ru in the present compound is consistent with the 1111 system.^{10,45} The other transition-metal impurities show less difference in suppression effects than Zn.

On the basis of previous pair-breaking analysis in the BaFe_{1.89-2x}Zn_{2x}Co_{0.11}As₂ superconductors,³⁰ we calculated the pair-breaking rate $\alpha = z\hbar\gamma/2\pi k_B T_{c0}$ for Ba_{0.5}K_{0.5}Fe_{2-2x}M_{2x}As₂ ($M = \text{Mn, Ru, Co, Ni, Cu, and Zn}$), where T_{c0} is the T_c of the impurity-free compound, and γ is the electron scattering rate. Previous theoretical study proposed a relation between γ and $\Delta\rho_0$ as $\Delta\rho_0$ ($\mu\Omega \text{ cm}$) = 0.18 γ (K) in terms of a five-orbital model for 122 systems; here $\Delta\rho_0$ is the difference of the residual resistivity between the impurity-doped and impurity-free crystals. For the s_{\pm} -wave state, the SC should vanish in the range $\alpha > \alpha_c^{\pm} = 0.22$.⁷ For the present experiment, we estimated $\alpha = 0.88z\Delta\rho_0/T_{c0}$ by

using $z = 0.50$ as shown in Fig. 9. The T_c/T_{c0} vs α data change is roughly linear; therefore we applied a linear function to the data and estimated the critical pair-breaking parameters as 6.52, 5.23, 4.24, 5.41, and 6.05 for impurities of Mn, Co, Ni, Cu, and Zn, respectively. A comparable result was obtained for the pair-breaking effect of Zn in the BaFe_{1.89-2x}Zn_{2x}Co_{0.11}As₂ superconductors as $\alpha = 11.49$ with $z = 0.5$. Recent data for proton-irradiated Ba(Fe,Co)₂As₂ show results similar to those of our chemical doping.⁴⁶ Obviously, the pair-breaking parameters experimentally estimated for the present compound are far above the limit $\alpha_c^{\pm} = 0.22$ for the s_{\pm} -wave model, suggesting the realization of the s_{++} -wave state rather than the s_{\pm} -wave model in the 122-type Fe-based superconductor.

V. CONCLUSIONS

To summarize, we have studied the superconductivity suppression effect on Ba_{0.5}K_{0.5}Fe_{2-2x}M_{2x}As₂ single crystals by substitution of transition metals ($M = \text{Mn, Ru, Co, Ni, Cu, and Zn}$). The superconductivity of the p -type iron-based superconductor is maintained robustly with the impurity Ru, and weakly with the impurities Mn, Co, Ni, Cu, and Zn, whose T_c suppression rates are 6.98, 1.73, 2.21, 2.68, and 2.22 K/%, respectively. Mn is observed as having the strongest suppression effects, while the other transition-metal impurities of Co, Ni, Cu, and Zn show similar suppression effects regardless of magnetic or nonmagnetic property. However, the present T_c suppression rate of both magnetic and nonmagnetic impurities remains much lower than what is expected for the s_{\pm} -wave model. The temperature dependence of resistivity data showed an obviously low- T upturn for the high-level impurity-doped crystals, which is due to the occurrence of localization. The relatively weak T_c suppression effects from Mn, Co, Ni, Cu, and Zn are considered to be a result of localization rather than the pair-breaking effect in the s_{\pm} -wave model. However, another scenario similar to the non-sign-reversal s -wave model (s_{++} wave) is more likely for the present superconductors.

ACKNOWLEDGMENTS

We thank M. Miyakawa for the high-pressure experiment and Dr. K. Kosuda for the EPMA experiment, and also thank D. Johrendt, H. B. Wang, B. Y. Zhu, M. Sato, and P. J. Pereira for valuable discussions. This research was supported in part by the World Premier International Research Center from MEXT, Grants-in-Aid for Scientific Research (22246083) from JSPS, and the Funding Program for World-Leading Innovative R&D on Science and Technology (FIRST Program) from JSPS.

*Li.Jun@nims.go.jp

¹Y. Kamihara, T. Watanabe, M. Hirano, and H. Hosono, *J. Am. Chem. Soc.* **130**, 3296 (2008).

²M. Rotter, M. Tegel, and D. Johrendt, *Phys. Rev. Lett.* **101**, 107006 (2008).

³Z. A. Ren, W. Lu, J. Yang, W. Yi, X. L. Shen, C. Zheng, G. C. Che, X. L. Dong, L. L. Sun, F. Zhou, and Z. X. Zhao, *Chin. Phys. Lett.* **25**, 2215 (2008).

⁴I. I. Mazin, D. J. Singh, M. D. Johannes, and M. H. Du, *Phys. Rev. Lett.* **101**, 057003 (2008).

⁵I. I. Mazin, *Nature* **464**, 183 (2010).

⁶K. Kuroki, S. Onari, R. Arita, H. Usui, Y. Tanaka, H. Kontani, and H. Aoki, *Phys. Rev. Lett.* **101**, 087004 (2008).

⁷S. Onari and H. Kontani, *Phys. Rev. Lett.* **103**, 177001 (2009).

⁸S. Onari, H. Kontani, and M. Sato, *Phys. Rev. B* **81**, 060504(R) (2010).

- ⁹T. Saito, S. Onari, and H. Kontani, *Phys. Rev. B* **82**, 144510 (2010).
- ¹⁰M. Sato, Y. Kobayashi, S. C. Lee, H. Takahashi, E. Satomi, and Y. Miura, *J. Phys. Soc. Jpn.* **79**, 014710 (2010).
- ¹¹D. V. Efremov, M. M. Korshunov, O. V. Dolgov, A. A. Golubov, and P. J. Hirschfeld, *Phys. Rev. B* **84**, 180512(R) (2011).
- ¹²P. J. Hirschfeld, M. M. Korshunov, and I. I. Mazin, *Rep. Prog. Phys.* **74**, 124508 (2011).
- ¹³W. Q. Chen, K.-Y. Yang, Y. Zhou, and F.-C. Zhang, *Phys. Rev. Lett.* **102**, 047006 (2009).
- ¹⁴S. Maiti, M. M. Korshunov, T. A. Maier, P. J. Hirschfeld, and A. V. Chubukov, *Phys. Rev. Lett.* **107**, 147002 (2011).
- ¹⁵P. W. Anderson, *J. Phys. Chem. Solids* **11**, 26 (1959).
- ¹⁶H. Alloul, J. Bobroff, M. Gabay, and P. J. Hirschfeld, *Rev. Mod. Phys.* **81**, 45 (2009).
- ¹⁷G. V. M. Williams, J. L. Tallon, and R. Dupree, *Phys. Rev. B* **61**, 4319 (2000).
- ¹⁸C. Bernhard, Ch. Niedermayer, T. Blasius, G. V. M. Williams, R. De Renzi, C. Bucci, and J. L. Tallon, *Phys. Rev. B* **58**, 8937 (1998).
- ¹⁹M.-H. Julien, T. Fehér, M. Horvatić, C. Berthier, O. N. Bakharev, P. Ségransan, G. Collin, and J.-F. Marucco, *Phys. Rev. Lett.* **84**, 3422 (2000).
- ²⁰J. M. Tarascon, E. Wang, S. Kivelson, B. G. Bagley, G. W. Hull, and R. Ramesh, *Phys. Rev. B* **42**, 218 (1990).
- ²¹N. P. Armitage, P. Fournier, and R. L. Greene, *Rev. Mod. Phys.* **82**, 2421 (2010).
- ²²J. L. Tallon, *Phys. Rev. B* **58**, 5956 (1998).
- ²³B. vom Hedt, W. Lisseck, K. Westerholt, and H. Bach, *Phys. Rev. B* **49**, 9898 (1994).
- ²⁴Y. K. Kuo, C. W. Schneider, M. J. Skove, M. V. Nevitt, G. X. Tessema, and J. J. McGee, *Phys. Rev. B* **56**, 6201 (1997).
- ²⁵P. Cheng, B. Shen, J. P. Hu, and H. H. Wen, *Phys. Rev. B* **81**, 174529 (2010).
- ²⁶Y. Li, J. Tong, Q. Tao, C. Feng, G. Cao, Z. Xu, W. Chen, and F. Zhang, *New J. Phys.* **12**, 083008 (2010).
- ²⁷Y. F. Guo, Y. G. Shi, S. Yu, A. A. Belik, Y. Matsushita, M. Tanaka, Y. Katsuya, K. Kobayashi, I. Nowik, I. Felner, V. P. S. Awana, K. Yamaura, and E. Takayama-Muromachi, *Phys. Rev. B* **82**, 054506 (2010).
- ²⁸D. Tan, C. Zhang, C. Xi, L. Ling, L. Zhang, W. Tong, Y. Yu, G. Feng, H. Yu, L. Pi, Z. Yang, S. Tan, and Y. Zhang, *Phys. Rev. B* **84**, 014502 (2011).
- ²⁹J. J. Li, Y. F. Guo, S. B. Zhang, S. Yu, Y. Tsujimoto, K. Yamaura, and E. Takayama-Muromachi, *Physica C* **471**, 213 (2011).
- ³⁰J. Li, Y. Guo, S. Zhang, S. Yu, Y. Tsujimoto, H. Kontani, K. Yamaura, and E. Takayama-Muromachi, *Phys. Rev. B* **84**, 020513(R) (2011).
- ³¹F. Han, X. Zhu, P. Cheng, G. Mu, Y. Jia, L. Fang, Y. Wang, H. Luo, B. Zeng, B. Shen, L. Shan, C. Ren, and H.-H. Wen, *Phys. Rev. B* **80**, 024506 (2009).
- ³²L. J. Zhang and D. J. Singh, *Phys. Rev. B* **80**, 214530 (2009).
- ³³J. M. Tarascon, P. Barboux, P. F. Miceli, L. H. Greene, G. W. Hull, M. Eibschutz, and S. A. Sunshine, *Phys. Rev. B* **37**, 7458 (1988).
- ³⁴E. Satomi, S. C. Lee, Y. Kobayashi, and M. Sato, *J. Phys. Soc. Jpn.* **79**, 094702 (2010).
- ³⁵S. C. Lee, E. Satomi, Y. Kobayashi, and M. Sato, *J. Phys. Soc. Jpn.* **79**, 023702 (2010).
- ³⁶J. Li, Y. Guo, S. Zhang, Y. Tsujimoto, X. Wang, C. I. Sathish, S. Yu, K. Yamaura, and E. Takayama-Muromachi, *Solid State Commun.* **152**, 671 (2012).
- ³⁷H. Kontani and M. Ohno, *Phys. Rev. B* **74**, 014406 (2006).
- ³⁸H. Q. Yuan, J. Singleton, F. F. Balakirev, S. A. Baily, G. F. Chen, J. L. Luo, and N. L. Wang, *Nature (London)* **457**, 565 (2009).
- ³⁹S. Nandi, M. G. Kim, A. Kreyssig, R. M. Fernandes, D. K. Pratt, A. Thaler, N. Ni, S. L. Bud'ko, P. C. Canfield, J. Schmalian, R. J. McQueeney, and A. I. Goldman, *Phys. Rev. Lett.* **104**, 057006 (2010).
- ⁴⁰N. Ni, M. E. Tillman, J.-Q. Yan, A. Kracher, S. T. Hannahs, S. L. Bud'ko, and P. C. Canfield, *Phys. Rev. B* **78**, 214515 (2008).
- ⁴¹M. K. Yu and J. P. Franck, *Phys. Rev. B* **48**, 13939 (1993).
- ⁴²K. Nakamura, R. Arita, and H. Ikeda, *Phys. Rev. B* **83**, 144512 (2011).
- ⁴³D. V. Evtushinsky, D. S. Inosov, V. B. Zabolotnyy, M. S. Viazovska, R. Khasanov, A. Amato, H.-H. Klauss, H. Luetkens, Ch. Niedermayer, G. L. Sun, V. Hinkov, C. T. Lin, A. Varykhalov, A. Koitzsch, M. Knupfer, B. Büchner, A. A. Kordyuk, and S. V. Borisenko, *New J. Phys.* **11**, 055069 (2009).
- ⁴⁴K. Nakayama, T. Sato, P. Richard, Y.-M. Xu, Y. Sekiba, S. Souma, G. F. Chen, J. L. Luo, N. L. Wang, H. Ding, and T. Takahashi, *Europhys. Lett.* **85**, 67002 (2009).
- ⁴⁵S. C. Lee, E. Satomi, Y. Kobayashi, and M. Sato, *J. Phys. Soc. Jpn.* **79**, 023702 (2010).
- ⁴⁶Y. Nakajima, T. Taen, Y. Tsuchiya, T. Tamegai, H. Kitamura, and T. Murakami, *Phys. Rev. B* **82**, 220504(R) (2010).